

Force sum rules, stress theorems, and Thomas-Fermi treatment of a 90° jellium edge

G. Schreckenbach,* R. Kaschner, and P. Ziesche†

Institut für Theoretische Physik, Technische Universität Dresden, 0-8027 Dresden, Germany

(Received 21 January 1992)

A quarter-space jellium or 90° jellium wedge is considered a highly idealized element of real metallic surfaces with ledges or with atomic-scale sharp edges such as those in quantum wires and quantum dots. Using the concept of energy density, an edge energy is defined. Force sum rules are summarized, relating the electric field that arises from the dipole layer along the background discontinuity with density derivatives of the surface energy (of a half-space jellium) and of the sharp edge energy. Within the Thomas-Fermi approximation, the electron density is determined. Besides sharp edges, nonsharp edges with finite curvature are also considered, the latter characterized by the recently introduced curvature energy.

I. INTRODUCTION

From a total-energy point of view, an ideal crystal is characterized by a bulk energy (per unit cell) and an ideal surface by a surface energy (per unit area). Recently there is increasing interest in regularly stepped (vicinal) surfaces with a periodic array of ledges or steps. A single ledge may be considered as a pair of edges, consisting of an “upper” one (90°) and a “lower” one (270°). Instead of directly calculating the characteristic energy of such a single ledge, we simplify this problem in a twofold way: (i) we get rid of the multicenter problem by replacing the system with a jellium model, and (ii) we consider first a single 90° edge only, i.e., a quarter-space-filling jellium. Such a 90° jellium wedge can be considered as an idealized model for atomic-scale sharp edges as they might appear at quantum wires or quantum dots. Long before the advent of quantum wires or dots, the 90° jellium wedge was treated by Kesmodel and Falicov theoretically in view of “the different chemical reactivity of metallic edges, corners and steps”; they determined the potential from an approximate model electron density.¹

Sharp edges are limiting cases of nonsharp edges, which are, in turn, examples of more general curved surfaces. The latter are finding recently more and more interest²⁻⁵ and are to be characterized by a curvature energy. We introduce the sharp edge energy to characterize the sharp jellium edge; to this end we make use of the concept of energy density.⁶ The desire to deal with a sharp jellium edge was also motivated by studying the surface stress theorem of half-space jellia and corresponding force sum rules,⁶⁻¹⁰ which can be easily derived from the local momentum balance for the quantum-mechanical stress field.^{6,11,12} Surprisingly, the stress parallel to the surface led us automatically to the need to consider a half-space jellium cleaved perpendicularly to its surface in such a way that one-half was shifted infinitely far away. Thus a quarter-space jellium is left with electrons spilled out and, following from this, an electric field, which causes Hellmann-Feynman forces on the (unrelaxed) background. We found that certain integrals (moments) of this Hellmann-Feynman force density are relat-

ed to density derivatives of the surface and the edge energies.

The paper is organized as follows. First we summarize the theorems, specify energy density and stress field for the gradient expansion approximation (GEA) of the density-functional theory (Sec. II). Then we present the solution of the problem within the Thomas-Fermi approximation (TFA): numerical procedure (Sec. III) and results (Sec. IV). Finally, an outlook is given (Sec. V).

II. JELLIUM EDGE AND FORCE SUM RULES

We consider a jellium with a background density

$$\rho(x,y) = n_0 \Theta(-x) \Theta(-y),$$

an electron density $n(x,y)$, and an electric field (times $|e|$)

$$\mathbf{E}(x,y) = -\partial\varphi(x,y)/\partial\mathbf{r}.$$

The latter arises from the dipole layer near the background discontinuity, i.e., at $x \approx 0$ ($y \leq 0$) and $y \approx 0$ ($x \leq 0$). The condition

$$\int dx \int dy [\rho(x,y) - n(x,y)] = 0$$

expresses the neutrality of the total system.

To define a characteristic edge energy for this system we use the concept of energy density^{4,6,7,13} which, within the GEA of the density-functional theory, takes the form^{14,15}

$$e(\mathbf{r}) = \frac{1}{2} \frac{[\mathbf{E}(\mathbf{r})]^2}{4\pi\epsilon^2} + g(n(\mathbf{r}), s(\mathbf{r})),$$

$$s(\mathbf{r}) = \frac{1}{2} \left[\frac{\partial n(\mathbf{r})}{\partial \mathbf{r}} \right]^2, \quad (1)$$

where $\epsilon^2 = e^2/4\pi\epsilon_0$ and $g(n,s)$ comprises both the kinetic-energy density $t(\mathbf{r})$ and the exchange and correlation (XC) part of the potential-energy density. The first term of $e(\mathbf{r})$ is the Hartree or electrostatic part of the potential-energy density. Local-density approximation means the neglect of density gradient terms

$$g(n,s) \approx g_0(n) = n\varepsilon(n),$$

with

$$\varepsilon(n) = t_0(n) + \varepsilon_{XC}(n),$$

the bulk energy (per particle) of the homogeneous jellium. $t_0(n)$ is the kinetic energy (per particle) of the corresponding noninteracting Fermi gas

$$t_0(n) = \frac{3}{5}\varepsilon_F, \quad \varepsilon_F = \frac{\hbar^2}{2m}k_F^2, \quad k_F^3 = 3\pi^2 n$$

and $\varepsilon_{XC}(n)$ is the XC energy of the homogeneous jellium.

The jellium wedge is characterized by the following asymptotic behavior. For $y \rightarrow -\infty$ the situation of a half-space jellium with background density $\rho(x)$ and characteristic quantities $n(x)$, $E(x)$, $e(x)$ arises: $n(x, -\infty) = n(x)$, $E_x(x, -\infty) = E(x)$, $E_y(x, -\infty) = 0$, $e(x, -\infty) = e(x)$. The corresponding statement is true for $x \rightarrow -\infty$: $n(-\infty, y) = n(y)$, $E_x(-\infty, y) = 0$, $E_y(-\infty, y) = E(y)$, $e(-\infty, y) = e(y)$. Besides this, $n(-\infty) = n_0$ and $e(-\infty) = n_0\varepsilon$ with $\varepsilon = \varepsilon(n_0)$. Now, keeping this behavior of $e(x)$ and $e(x,y)$ in mind, the surface energy ε^s and the sharp edge energy ε^e can be defined as⁶⁻⁸

$$\varepsilon^s = \int dx [e(x) - \Theta(-x)n_0\varepsilon], \quad (2)$$

$$\varepsilon^e = \int dx \int dy [e(x,y) - \Theta(-x)e(y) - \Theta(-y)e(x) + \Theta(-x)\Theta(-y)n_0\varepsilon]. \quad (3)$$

The following Hellmann-Feynman force sum rules can be proved:

$$n_0 \frac{d}{dn_0} \varepsilon = \int_{-\infty}^0 dx E(x), \quad (4)$$

$$n_0 \frac{d}{dn_0} \varepsilon^s = n_0 \int_{-\infty}^0 dx xE(x), \quad (5)$$

$$\left[n_0 \frac{d}{dn_0} - 1 \right] \varepsilon^s = n_0 \int_{-\infty}^0 dx \int_{-\infty}^0 dy [E_x(x,y) - E(x)], \quad (6)$$

$$n_0 \frac{d}{dn_0} \varepsilon^e = n_0 \int_{-\infty}^0 dx \int_{-\infty}^0 dy x [E_x(x,y) - E(x)] \quad (7)$$

(see Refs. 7-9, 16, and 17). Equation (4) is a "bulk-surface theorem," Eq. (5) is a "surface-surface theorem," Eq. (6) is a "surface-edge theorem," and Eq. (7) is an "edge-edge theorem." In addition to the force sum rules (5) and (6), the surface stress theorem holds^{12,14,15,18} which, within GEA, takes the form

$$n_0 \frac{d}{dn_0} \varepsilon^s = \int dx \left\{ -\frac{1}{2} \frac{E^2(x)}{4\pi\epsilon^2} + \left[n^2 \frac{d\varepsilon}{dn} - n(n'g_s)' + (n')^2 g_s \right]_{n(x)} - \Theta(-x)n_0^2 \frac{d\varepsilon}{dn_0} \right\}, \quad (8)$$

$$\left[n_0 \frac{d}{dn_0} - 1 \right] \varepsilon^s = \int dx \left\{ +\frac{1}{2} \frac{E^2(x)}{4\pi\epsilon^2} + \left[n^2 \frac{d\varepsilon}{dn} - n(n'g_s)' \right]_{n(x)} - \Theta(-x)n_0^2 \frac{d\varepsilon}{dn_0} \right\}. \quad (9)$$

On the right-hand sides of Eqs. (8) and (9), the concept of quantum-mechanical stress fields is used.^{6,11,12} While the weighted sum, i.e., twice (9) plus (8) (note that this is just the trace of the surface stress), gives the surface virial theorem, the difference of Eqs. (8) and (9) yields an expression (a sum rule) for the surface energy:

$$\varepsilon^s = \int dx \left[-\frac{E^2(x)}{4\pi\epsilon^2} + (n')^2 g_s \right]_{n(x)}. \quad (10)$$

From this it can be seen that in the lowest order of the GEA, i.e., $g_s \approx 0$ or $g \approx g_0$, the surface energy is always negative. For comparison, within the Kohn-Sham treatment due to Lang and Kohn,¹⁹ $\varepsilon^s < 0$ only for $r_s \lesssim 2$. Similarly as in Eqs. (8) and (9), the density derivative of the edge energy is related to integrals of the edge-stress field [which, within GEA, is determined by $g(n,s)$ and $E(x,y), n(x,y)$] (edge-stress theorem⁸).

To obtain $n(x,y)$, the electron distribution of a jellium wedge, one has to solve the corresponding Euler and Poisson equations under the constraint of fixed $\rho(x,y)$ and the neutrality condition. (The analogous interface problem is studied in Refs. 15 and 18.)

III. THOMAS-FERMI CALCULATION

As a first calculational step, we treated the TFA, which is a special case of the GEA, corresponding to $g \approx g_0$ and furthermore to $\varepsilon \approx t_0$, i.e., $\varepsilon_{XC} \approx 0$. We solved the coupled system of Thomas-Fermi (Euler) and Poisson equations

$$\frac{\hbar^2}{2m} [3\pi^2 n(x,y)]^{2/3} - \varphi(x,y) = 0, \quad (11)$$

$$-\Delta\varphi(x,y) = 4\pi\epsilon^2 [\rho(x,y) - n(x,y)], \quad (12)$$

directly numerically.²⁰ This numerical solution consists of the following steps.

(i) With the abbreviation

$$C = \frac{4\epsilon^2}{3\pi} \left[\frac{2m}{\hbar^2} \right]^{3/2},$$

an appropriate scaling

$$\varphi_0 = \left[\frac{4\pi\epsilon^2 n_0}{C} \right]^{2/3} \quad \text{and} \quad l_0 = (C\varphi_0^{1/2})^{-1/2}$$

is introduced which, in terms of atomic units ($a_0 = \hbar^2/m\epsilon^2$), is given by

$$\varphi_0 = \frac{1}{2} \left[\frac{9\pi}{4} \right]^{2/3} \frac{1}{r_s^2} \frac{\epsilon^2}{a_0} \quad (13)$$

and

$$l_0 = \frac{1}{2} \left[\frac{3\pi^2}{2} \right]^{1/6} r_s^{1/2} a_0. \quad (14)$$

The dimensionless equation for $\varphi(x,y)$ then reads

$$\bar{\Delta}\bar{\varphi} = \bar{\varphi}^{3/2} - \Theta(-\bar{x})\Theta(-\bar{y}) \quad (15)$$

with $\bar{\varphi} = \varphi/\varphi_0$, $\bar{x} = x/l_0$, $\bar{y} = y/l_0$, and $\bar{\Delta} = l_0^2 \Delta$.

(ii) Coordinates

$$\xi = \frac{2}{\pi} \arctan \bar{x}, \quad \eta = \frac{2}{\pi} \arctan \bar{y}$$

are introduced, which vary only between -1 and $+1$. So we obtain from (15) a (little more complicated) differential equation for $\bar{\varphi}(\xi, \eta)$, with the boundary conditions $\bar{\varphi}(\xi, \eta) = \bar{\varphi}(\eta, \xi)$, $\bar{\varphi}(-1, -1) = 1$, $\bar{\varphi}(+1, +1) = 0$, $\bar{\varphi}(-1, \eta) = \bar{\varphi}_{MR}(\eta)$, and $\bar{\varphi}(\xi, -1) = \bar{\varphi}_{MR}(\xi)$, where $\bar{\varphi}_{MR}$ is the (dimensionless) potential of a half-space jellium, which is known for the TFA in analytical form.²¹

(iii) Discretization of the ξ and η intervals. The differential equation for $\bar{\varphi}(\xi, \eta)$ is transferred by means of three-point formulas into a set of nonlinear algebraic equations for the values $\bar{\varphi}(\xi_i, \eta_j)$ at the mesh points in the ξ - η plane with

$$\xi_i, \eta_i = -1 + 2(i-1)/(N-1),$$

$i = 1, \dots, N$. N is chosen between 31 and 101.

(iv) The solution of this system of algebraic equations is accomplished with the boundary conditions of (ii) by means of a Newton-Raphson method where, for each Newton-Raphson step, the relaxation method of Southwell (because of the large matrices) and a mixing procedure are applied. The Newton-Raphson iteration is started with

$$\bar{\varphi}(\xi, \eta) = \bar{\varphi}_{MR}(\xi)\bar{\varphi}_{MR}(\eta).$$

This is an expression similar to the approximation for $n(x,y)$ used in Ref. 1 [their Eq. (3)].

IV. RESULTS

(i) *Electron density and potential.* The numerical accuracies of $\bar{\varphi}$ that are obtained are 10^{-4} for $N=51$ and 10^{-2} for $N=101$, but the plots $\bar{\varphi}(\bar{x}, \bar{y})$ practically agree for both cases. Such a plot of the scaled potential $\bar{\varphi}(\bar{x}, \bar{y})$ is shown in Fig. 1. From these "universal" curves, the electronic density $n(x,y)$ can be obtained according to Eq. (11) via

$$n(x,y) = n_0 [\bar{\varphi}(x/l_0, y/l_0)]^{3/2}.$$

Friedel oscillations are not present as a consequence of the TFA.

(ii) *Sum rules.* We tested the sum rules (5)–(9). The results for $r_s=1$ are presented in Table I with $N=101$ for the first two lines. The values found in the last line of Table I are obtained when $N=51$; if $N=101$ is chosen, then the values 0.017 and 0.036, respectively, are obtained, indicating that insufficiently accurate values of $\mathbf{E}(x,y)$ are obtained for this choice of N . Note that for other values of r_s the numbers of Table I are to be scaled

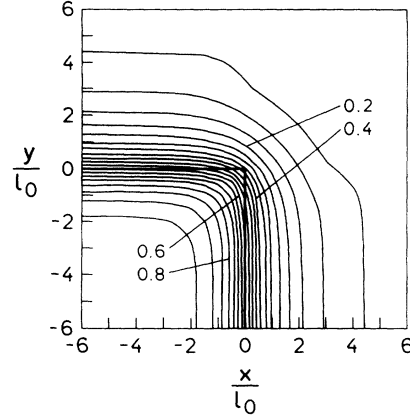


FIG. 1. Universal contour plot of the scaled electrostatic potential (times $|e|$) $\bar{\varphi}(\bar{x}, \bar{y})$ for a quarter-space jellium with background density $n_0\Theta(-x)\Theta(-y)$ in TFA. Note that $\varphi(x,y;r_s) = \varphi_0\bar{\varphi}(x/l_0, y/l_0)$.

only; this is a consequence of the r_s scaling of φ_0 and l_0 according to Eqs. (13) and (14).

(iii) *Edge energy.* For the sharp edge energy (3), via (1) within TFA we obtained a simple scaling with r_s

$$\epsilon^e = \frac{0.045}{r_s^4} \frac{\text{Ry}}{a_0} = \frac{0.61}{r_s^4} \frac{\text{eV}}{a_0}. \quad (16)$$

Recently, Perdew and co-workers^{3,4} studied curved surfaces like jellium spheres and spherical voids with the aim of estimating vacancy formation energies. They introduced, in addition to the known bulk and surface energies, a curvature energy via the total energy E of an extended system of volume V and surface S :

$$E = n_0 \epsilon V + \epsilon^s S + \gamma \frac{1}{2} \int \frac{dS}{R}. \quad (17)$$

R is the local curvature of the surface-area element dS , with $R^{-1} = \frac{1}{2}(R_1^{-1} + R_2^{-1})$, where R_1 and R_2 refer to the principal axes. Within TFA,

$$\gamma = - \frac{0.46}{r_s^4} \frac{\text{eV}}{a_0}$$

results; within GEA, Engel and Perdew obtained, for $r_s=2, 4$, and 6 , the values $\gamma=0.04, 0.01$, and 0.002 eV/ a_0 , respectively.³ For a nonsharp edge with the curvature radii $R_1 < \infty$ and $R_2 \rightarrow \infty$, the last term of Eq. (17) results in $\gamma(\pi/8)L$, with L being the edge length. While Eq. (17) holds for large R_1 (Ref. 22) the limiting case of a sharp edge ($R_1 \rightarrow 0$) is described by²³

TABLE I. Test of the sum rules, Eqs. (5)–(9), for $r_s=1$. lhs and rhs denote left- and right-hand sides, respectively.

Eq.	lhs	rhs
(5)	-0.229 1	-0.229 3
(6)	-0.076 35	-0.078 92
(7)	0.013 4	0.013 2
(8)		-0.229 0
(9)		-0.076 35

$$E = n_0 \epsilon V + \epsilon^e S + \epsilon^e L . \quad (18)$$

While in Eq. (17) terms $O(1/R_1)$ are omitted, in Eq. (18) terms $O(R_1)$ are left out. Thus γ and ϵ^e are different quantities.²⁴

V. OUTLOOK

Because the TFA is a rather poor approximation, one should perform Lang-Kohn-type calculations for a 90° jellium wedge to have a reference system for extended quarter-space crystals, just as with the Lang-Kohn data for planar metallic surfaces. To this end Eqs. (1), (8), and (9) must be replaced by the corresponding Kohn-Sham expressions.^{6,10,11} Self-consistent solutions of the Kohn-Sham equation for the jellium wedge should confirm (or correct) the enhancement of Friedel oscillations, which has been stressed by Kesmodel and Falicov.¹ It should also be of interest to study how the results change if stabilized jellium^{4,25,26} or nonsharp edges are considered. Next, the lattice structure via pseudopotentials should be

taken into account, as this has been done similarly for surfaces.^{19,27}

Recently, electronic-structure calculations have been published for a single step at an aluminum surface²⁸ and for stepped metal surfaces [relaxation of the Al(331) surface].²⁹ Within the jellium model, the electron density has been determined approximately for a single step on a jellium surface with the help of an appropriate ansatz³⁰ and self-consistently for the stepped jellium surface.³¹ It remains (among other things) to derive from such calculations characteristic step energies. Another interesting problem is the stress field surrounding a wedge.³²

ACKNOWLEDGMENTS

The authors are grateful to J. P. Perdew, A. Liebsch, E. Mrosan, and H. Wonn for stimulating discussions. One of us (P.Z.) would like to thank Professor P. Fulde and the Max-Planck-Institute für Festkörperforschung, Stuttgart, for their hospitality.

*Present address: Department of Chemistry, University of Calgary, Calgary, Alberta, Canada T2 N1 N4.

[†]Present address: Gubener Strasse 48, D-O-8036 Dresden, Germany.

¹L. L. Kesmodel and L. M. Falicov, *Solid State Commun.* **16**, 1201 (1975).

²V. V. Pogosov, *Solid State Commun.* **75**, 469 (1990).

³J. P. Perdew, Y. Wang, and E. Engel, *Phys. Rev. Lett.* **66**, 508 (1991); E. Engel and J. P. Perdew, *Phys. Rev. B* **43**, 1331 (1991).

⁴C. Fiolhais and J. P. Perdew, *Phys. Rev. B* **45**, 6207 (1992).

⁵M. Seidl, M. E. Spina, and M. Brack, *Z. Phys. D* **19**, 101 (1991).

⁶P. Ziesche, *Ann. Phys. (Leipzig)* **45**, 626 (1988).

⁷R. Kaschner and P. Ziesche (unpublished).

⁸R. Kaschner, Ph.D. thesis, Technische Universität Dresden, 1989.

⁹P. Ziesche and R. Kaschner, *Solid State Commun.* **78**, 703 (1991); see also *Phys. Status Solidi B* **145**, K9 (1988).

¹⁰P. Ziesche and J. Gräfenstein, *Phys. Rev. B* **46**, 1715 (1992).

¹¹P. Ziesche, J. Gräfenstein, and O. H. Nielsen, *Phys. Rev. B* **37**, 8167 (1988).

¹²Yu. A. Uspenski, P. Ziesche, and J. Gräfenstein, *Z. Phys. B* **76**, 193 (1989).

¹³N. Chetty and R. M. Martin, *Phys. Rev. B* **45**, 6074 (1992).

¹⁴R. Kaschner, J. Gräfenstein, and P. Ziesche (unpublished).

¹⁵P. Ziesche, R. Kaschner, and N. Nafari, *Phys. Rev. B* **41**, 10 553 (1990).

¹⁶H. F. Budd and J. Vannimenus, *Phys. Rev. Lett.* **31**, 1218

(1973); **31**, 1430 (1973).

¹⁷J. Vannimenus and H. F. Budd, *Solid State Commun.* **15**, 1739 (1974).

¹⁸P. Ziesche and R. Kaschner, *Physica B* **172**, 299 (1991).

¹⁹N. D. Lang and W. Kohn, *Phys. Rev. B* **1**, 4555 (1970).

²⁰G. Schreckenbach (unpublished).

²¹B. Mrowka and A. Recknagel, *Phys. Z.* **38**, 758 (1937).

²²One should expect $R_1 > r_s a_0$ [J. P. Perdew (private communication)].

²³D. Lehmann and P. Ziesche, *Helv. Phys. Acta* **57**, 621 (1984).

²⁴The relation between ϵ^e and γ guessed at in G. Schreckenbach, R. Kaschner, and P. Ziesche [see *Electronic Structure of Solids '91*, edited by P. Ziesche and H. Eschrig (Akademie Verlag, Berlin, 1991), p. 172] is withdrawn herewith. In terms of an R -dependent edge energy ϵ_R^e it is $\epsilon_R^e = \epsilon^e + O(R)$ and $\epsilon_R^e = (\pi/8)\gamma + O(1/R)$ for small and large R , respectively.

²⁵J. P. Perdew, H. Q. Tran, and E. D. Smith, *Phys. Rev. B* **42**, 11 627 (1990).

²⁶H. B. Shore and J. H. Rose, *Phys. Rev. Lett.* **66**, 2519 (1991).

²⁷R. Monnier and J. P. Perdew, *Phys. Rev. B* **17**, 2595 (1978).

²⁸R. Stumpf and M. Scheffler (unpublished).

²⁹J. S. Nelson and P. J. Feibelman, *Phys. Rev. Lett.* **68**, 2188 (1992).

³⁰M. D. Thompson and H. B. Huntington, *Surf. Sci.* **116**, 522 (1982).

³¹H. Ishida and A. Liebsch, *Phys. Rev. B* (to be published).

³²R. C. Ball and R. Blumenfeld, *Phys. Rev. Lett.* **65**, 1784 (1990); M. Marder, *ibid.* **68**, 2253 (1992).